HEFAT2014
10th International Conference on Heat Transfer, Fluid Mechanics and Thermodynamics
14 – 16 July 2014
Orlando, Florida

Final

ENHANCING GAS SEPRATION ACROSS A MEMBRANE WITH PULSATING FLOW

Nawaf Alkhamis, Dennis E. Oztekin, Ali E. Anqi, Abdulmohsen Alsaiari and Alparslan Oztekin*

*Author for correspondence
Dept. of Mechanical Engineering & Mechanics
Lehigh University
Bethlehem, PA 18015
USA
E-mail: alo2@lehigh.edu

ABSTRACT

Gas-gas separation is a critical process in natural gas purification. Removing acidic gasses from natural gas is particularly important to protect the pipeline from corrosion. Using a membrane to purify natural gas is receiving a lot of attention recently. Membrane performance can be enhanced by either improving the permeability or the selectivity of the membrane or by enhancing the momentum mixing in the bulk flow. Our work will focus on improving membrane performance by enhancing momentum mixing in the bulk flow for gas-gas separation to purify natural gas. Pulsating flow in a channel with turbulators will be considered. Computational fluid dynamics simulation will be conducted for turbulent flow of multicomponent fluid including mass transfer of each species. RANS - Reynolds-Averaged Navier-Stokes equation along with mass transport equation will be employed to simulate 2-D transient turbulent flows of bulk fluid. The membrane will be modeled as a functional surface where the flux of each component will be determined based on the local partial pressure of each species, composition, and permeability and selectivity of the membrane. The performance of the system will be measured by maximum mass separation with minimal frictional losses.

INTRODUCTION

Natural gas supplies nearly 24% of the world's energy consumption and it is predicted by the International Energy Agency that the demand for natural gas will grow by approximately 43% through 2035. The large demand for natural gas has motivated more study into the classical problem of extraction and transport. In this study the problem of effectively removing impurities in natural gas will be addressed. Natural gas extracted has 10% to 30% impurities. Raw natural gas contains ethane, propane, butane, water vapor and acidic gases such as carbon dioxide and hydrogen sulphide. The acid gasses and water vapor are dangerous as they cause corrosion in the natural gas pipelines. To protect the pipelines these impurities need to be minimized. The conventional method of removing water vapor from natural gas is by running the gas through a Glycol dehydration plant. Similarly amine gas treatment is the method of removing the acidic gases. These processes are not cost effective.

An alternative method for purifying natural gas is through the use of membrane technology [1]. Membrane technology has been investigated to a great extent and several ways to improve this method have been developed. Some approaches include: improving the permeability and selectivity of the membrane [2-6]; operating the membrane at optimum temperature and pressure [7-9]; or improving the separation module(s) [10]. Yet another approach to improve membrane performance is to enhance the turbulent mixing in the bulk flow. Enhancing turbulence to improve membrane performance has been studied extensively in the context of Reverse Osmosis and in the food industry [11-23]. However, the effect of turbulent pulsating flow and the effect of the vortex shedding on the membrane performance in gas-gas separation is not studied.

In a past study the present investigators studied the effect of spacers on multicomponent flows of CH_4 and CO_2 in a channel bounded by two membranes [24]. It was concluded that the presence of spacers, which introducing turbulent mixing, improves the effectiveness of the membrane. In the present study the effects of unsteady pulsation upstream of the flow is studied. A *k-ω* turbulent model, which includes unsteady effects, is employed to characterize the flow. The CO_2

absorption and CH_4 loss through the membrane are calculated and compared with results in a flow without pulsation.

NOMENCLATURE

A	surface area
C	concentration
D	mass diffusivity
J	mass flux through the membrane
L	channel length
P	permeability
Re	Reynolds Number
Sc	Schmidt number
U	Average velocity at the inlet
V_w	velocity on the membrane at y direction
d_c	spacer diameter
k	turbulent kinetic energy
h	channel height
l	membrane thickness
m	mass
p	pressure
u	x-component of the velocity
v	y-component of the velocity
x	x-direction
y	y-direction
υ	kinematic viscosity
ρ	density
α	selectivity
ω	specific dissipation rate
%m	percentage of the mass absorbed
f	frequency of pulsation at inlet
a	amplitude of pulsation at inlet

Subscripts

a	species: CO_2 or CH_4
b	species: CO_2 or CH_4
a/b	ratio of properties of a to properties of b
j,i	x- and y- directions
CO_2	properties of CO_2
CH_4	properties of CH_4
w	properties on the surface of membrane
T	eddy properties

GOVERNING EQUATIONS

Two dimensional flows in a channel bounded by two parallel membranes with unsteady pulsations in the inlet velocity are studied here for Reynolds number of 800. The aspect ratio of the computational domain is 120 (L/h) where L is the channel length and h is the gap between two parallel membranes. The Reynolds number based on the inlet condition is $Re = Uh/\upsilon$ with U is the average fluid speed and υ is the kinematic viscosity.

The flow at the inlet is periodically changing in time. The frequency is set as f and the amplitude of the pulsation is said to be a. Equations governing the fluid motion inside the channel between membranes are Navier-Stokes equation

$$\frac{\partial u_i}{\partial x_i} = 0 \tag{1}$$

$$\frac{\partial u_i}{\partial t} + u_j \frac{\partial u_i}{\partial x_j} = -\frac{1}{\rho}\frac{\partial p}{\partial x_i} + \nu \frac{\partial^2 u_i}{\partial x_j \partial x_j} \tag{2}$$

Here u_i is the fluid velocity vector, p is the pressure, x_i is the spatial coordinate, t is the time and $\rho = C_{CO2}\,\rho_{CO2} + C_{CH4}\,\rho_{CH4}$ is the density of the binary mixture with $C_{CO2,}\ \rho_{CO2}$ and $C_{CH4,}\ \rho_{CH4}$ are the concentration and the density of CO_2 and CH_4, respectively. $x \equiv x_1$ is the stream-wise direction, $x \equiv x_2$ is the span-wise direction, $u \equiv u_1$ is the stream-wise component of the velocity vector and $u \equiv u_2$ is the span-wise component of the velocity vector. The density of the mixture is assumed to be constant and calculated using the concentration of the species at the inlet. Species equation is of the form:

$$\frac{\partial C_a}{\partial t} + u_j \frac{\partial C_a}{\partial x_j} = D \frac{\partial^2 C_a}{\partial x_j \partial x_j} \tag{3}$$

D is the diffusion coefficient and C_a is the concentration of species "a" in a binary mixture of CH_4 and CO_2.

k-ω turbulent modeling is employed to simulate flow past arrays of spacers

$$\frac{\partial u}{\partial t} + u_j \frac{\partial u_i}{\partial x_j} = -\frac{1}{\rho}\frac{\partial p}{\partial x} + \frac{\partial}{\partial y}\left((\nu + \upsilon_T)\frac{\partial u}{\partial y}\right) \tag{4}$$

where $u = u_1$, $x = x_1$ and $y = x_2$. υ_T is the eddy viscosity and is determined using the k-ω model.

$$\frac{\partial k}{\partial t} + u_j \frac{\partial k}{\partial x_j} = -\frac{1}{\rho}\frac{\partial}{\partial y}\left((\nu + \sigma\upsilon_T)\frac{\partial k}{\partial y}\right) + \frac{\partial}{\partial y}\left(\upsilon\frac{\partial u}{\partial y}\right) - \beta k\omega \tag{5}$$

$$\frac{\partial \omega}{\partial t} + u_j \frac{\partial \omega}{\partial x_j} = -\frac{1}{\rho}\frac{\partial}{\partial y}\left((\nu + \sigma\upsilon_T)\frac{\partial \omega}{\partial y}\right) + \frac{\partial}{\partial y}\left(\upsilon\frac{\partial u}{\partial y}\right) - \beta\omega^2 \tag{6}$$

Here k is the turbulent kinetic energy and ω is the specific dissipation rate. The constants are selected to be $\sigma = 1$ and $\beta = 0.09$. Species equation for the k-ω model is of the form:

$$\frac{\partial C_a}{\partial t} + u_j \frac{\partial C_a}{\partial x_j} = \frac{\partial}{\partial y}\left((D + \sigma D_T)\frac{\partial \omega}{\partial y}\right) + \frac{\partial}{\partial y}\left(D\frac{\partial C_a}{\partial y}\right) - Sc_T\beta\omega \tag{7}$$

where D_T is the eddy diffusion coefficient and Sc_T is the turbulent Schmidt number. Sc_T is selected to be 0.85 in the present work.

On the surface of the membrane, the no-slip boundary condition is imposed on the velocity field with the suction rate (y-component of the velocity) calculated from local pressure and concentration. The mass flux of species "a" through a membrane is given by

$$J_a = \frac{P_a}{l}\left(p_a^{(1)} - p_a^{(2)}\right) \tag{8}$$

where J_a is the volume flux of species "a" per unit area extracted from the feed flow, l is the thickness of the membrane, P_a is the permeability of species "a", $\Delta p_a = \left(p_a^{(1)} - p_a^{(2)}\right)$ is the partial pressure difference of species "a" across the membrane. Species "a" can be either CO_2 or CH_4.

The suction rate on the surface of the membrane can be determined as

$$V_w = J_{CO_2} + J_{CH_4} = \frac{P_{CO_2}}{l}\left[\alpha \Delta p_{tot} + (1-\alpha)\Delta p_{CO_2}\right] \qquad (9)$$

where V_w is the suction rate. The selectivity of the membrane, $\alpha = P_{CH4}/P_{CO2}$, is defined as the ratio of the permeability of the species. Total pressure of the mixture $\Delta p_{tot} = \Delta p_{CH4} + \Delta p_{CO2}$

The concentration at the membrane wall is determined from [12,15-18,23]

$$D\frac{\partial C_a}{\partial y} = V_w C_a\left(1 - \frac{1}{\alpha}\right) \qquad (12)$$

The membrane performance is determined by the amount of CO_2 absorbed by the membrane and the amount of CH_4 which is lost through the membrane during the process.

Commercial software, CFX, is employed to solve the momentum, continuity, and mass transport equations. The k-ω turbulence models for flows in channels with spacers are used for Reynolds number of 800. The diffusion coefficient for CO_2 and CH_4 is $1.9\text{x}10^{-5}$ m^2/s. The concentration of CH_4 at the inlet is selected to be 0.7. The permeability of the membrane for CO_2 is $6.8\text{x}10^{-9}$ gpu and the selectivity is 0.0086. In order to ensure spectral convergence, simulations are conducted using $1.2\text{x}10^6$, $1.7\text{x}10^6$, and $2.1\text{x}10^6$ cells. The flow and concentration fields are nearly identical for all meshes selected. All the results presented in the present study are obtained using $1.2\text{x}10^6$ cells. The time step is selected as $2.5\text{x}10^{-5}$s; providing fifty discrete points in time to every periods of the vortex shedding.

GEOMETRY

Flow geometry consists of seventeen circular cross-sectioned spacers. They are arrayed with their origins placed at the mid-plane between the membranes, as shown in Figure 1. For the Reynolds number selected (Re = 800) the temporal and spatial structures of the flow will be dominated by the vortices shed from cylinders.

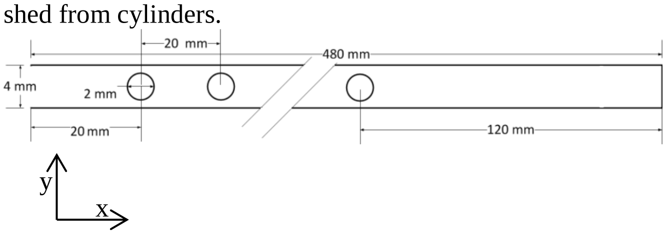

Figure 1 Schematic of the flow channel with arrayed spacers

RESULTS AND DISCUSSION

The lift force exerted by the fluid on the cylinder at the first row is depicted in Figure 2 for three different pulsating frequencies at Re = 800. The fact that the frequency of the fluctuations of the lift force is nearly the same for all three cases implies that the lift force is dominated by the vortex shedding. For no pulsation the Strouhal number (dimensionless frequency) is predicted to be about 0.2, which matches with those reported in the literature. These results also clearly show that the frequency of the vortex shedding is hardly influenced by the periodic flow imposed at the inlet.

For the pulsating and the steady flow at the inlet, suction from the membrane surface results in continual decrease of the mass flow rate through the channel. Since both membranes have the same functionality, the time-averaged velocity field is symmetric about the mid-point of the channel. The periodically alternating vortex shedding from top and bottom regions of the rear stagnation point causes flow asymmetric at any instant. Starting with the uniform 70% CH_4 concentration at the inlet, the mixture becomes richer with the CH_4 away from the inlet. Both CO_2 and CH_4 are absorbed from the mixture in the channel by the membrane. The absorption of CO_2 exceeds that of the CH_4, which leads to the richer CH_4 concentration.

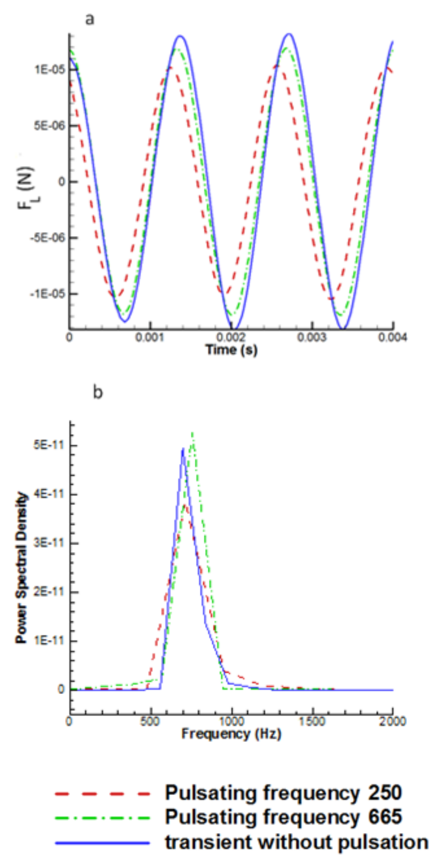

Figure 2 a) Lift force vs time and b) the power spectral density of the lift force

The velocity and concentration fields near spacers are obtained by employing turbulent modeling for *Re* = 800. Figure 3 shows the velocity vectors and the contours of the concentration of CO_2. The Kármán vortex shedding is dominating the flow and concentration field in the wake of spacers. The transient simulation conducted here predicts flow structures caused by the vortex shedding from the spacer for three different pulsation frequencies (0 Hz, 250 Hz and 665 Hz). Mixing caused by the vortex shedding is expected to enhance the membrane performance.

In order to determine membrane performance, the percentage mass change of the CO_2 absorbed and the CH_4 lost is determined from

$$\%M_a = \frac{M_{a,in} - M_{a,out}}{M_{a,in}} 100 \tag{13}$$

Here M_a is the mass of species "a" in a binary mixture of CH_4 and CO_2. The subscripts "in" and "out" denote the mass of each species at the inlet and the outlet of the channel.

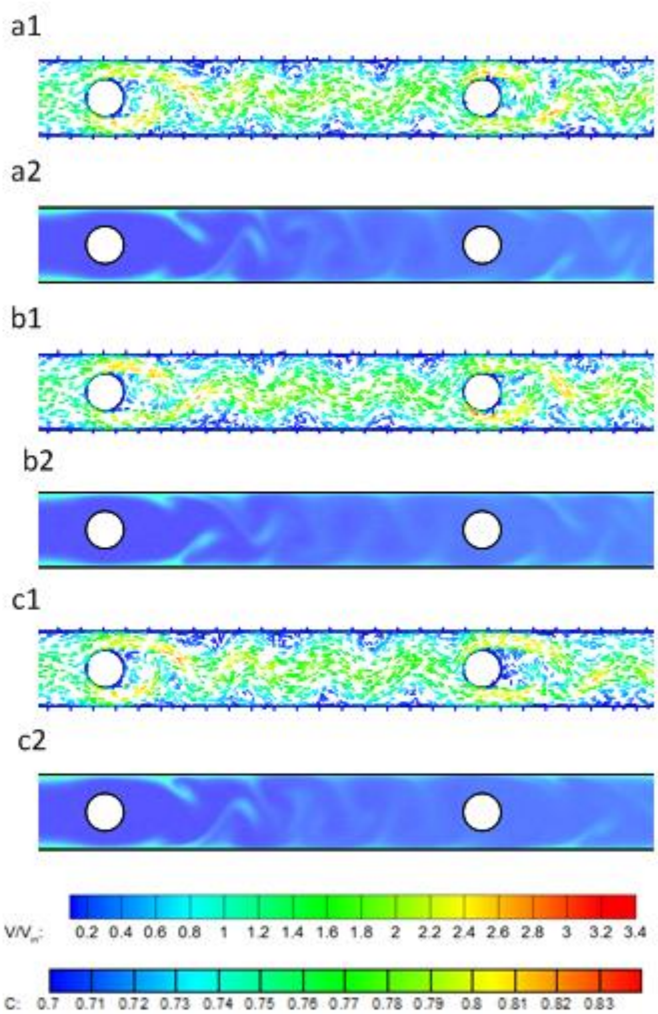

Figure 3 Velocity vectors (1) and contours of concentration of CO_2 (2) at *Re* = 800 for pulsation frequency of a) 665 Hz, b) 250 Hz and c) 0 Hz

Figure 4 depicts the percentage change mass of CO_2 and CH_4 between the inlet and the exit of the channel for *Re* = 800 for all three pulsating frequencies. The solid line denotes the steady state and transient simulations without the pulsation at the inlet. Obviously the effects of the vortex shedding on the CO_2 extracted through the membrane are captured by the time averaged representation obtained directly from the steady state simulations. The red and green lines in Figure 4 denote the percentage change mass of CO_2 for pulsating flow at the inlet with 250 Hz and the 665 Hz frequencies, respectively. They vary with time with the same frequency of pulsation. The average of percentage mass change is slightly lowered compared to the no pulsation case. As the pulsation frequency increases the time average of the mass percentage decreases.

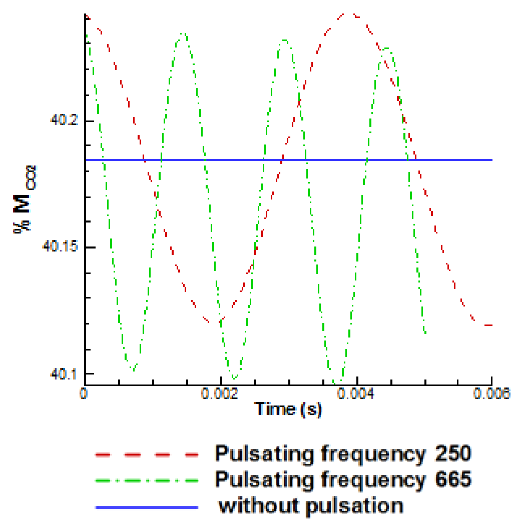

Figure 4 Percentage mass of CO_2 extracted through membrane at *Re* = 800 for different pulsating frequency at the inlet.

Figure 5 shows the Sherwood number right behind the first cylinder (d/x = 5.5), middle point between the first and the second cylinder (d/x = 7.5) and the right before the second cylinder (d/x = 9.5) as a function of time. The Sherwood number is periodic in time at all locations for all three cases; following the frequency of vortex shedding in each case, as shown in Figure 5. The average value of the Sherwood number right behind the cylinder is nearly the same for all cases, while the Sherwood number is higher in the middle of the cylinders and the front of the cylinders at lower frequencies. The mass flux at the surface of the membrane is strongly influenced by the nature of the vortex shedding at this Reynolds number of 800.

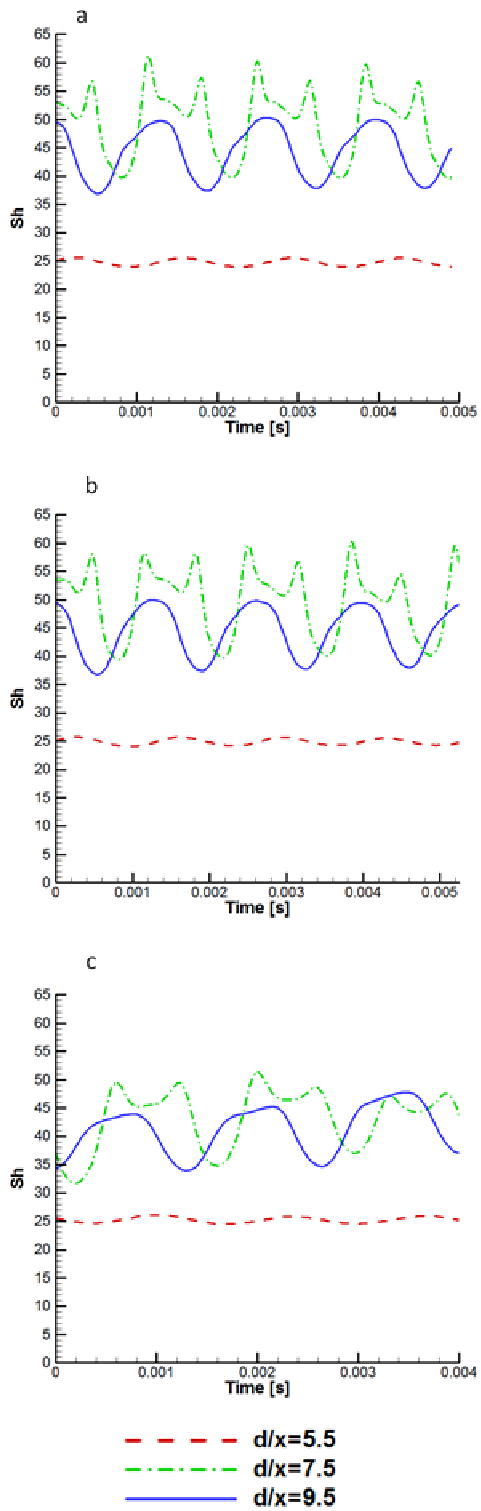

Figure 5 Sherwood number vs time at *Re* = 800 for pulsating frequency at the inlet a) 0 Hz, b) 250 Hz and c) 665 Hz.

CONCLUSION

Multicomponent flow of CH_4 and CO_2 in a channel bounded by two membranes is examined at *Re* = 800 for three different pulsating frequencies applied at the inlet. Flow simulations are conducted with the spacers. The *k*-*ω* model is used to predict the turbulent flow characteristics in the channel with the arrayed spacers. The presence of the spacers results in the vortex shedding that dominates the flow and concentration fields in all three cases. The Sherwood number is increased significantly compared to the case with no spacer due to momentum mixing caused by the vortex shedding. The frequency of the vortex shedding is nearly the same for all three cases studied here.

ACKNOWLEDGMENTS

The authors would like to acknowledge the support of Saudi government for the scholarship provided for NA, AA and AA.

REFERENCE

[1] Baker, R. W., and Lokhandwala, K., 2008, "Natural Gas Processing with Membranes: An Overview," Industrial & Engineering Chemistry Research, 47(7), pp. 2109-2121.

[2] Palomino, M., Corma, A., Jorda, J. L., Rey, F., and Valencia, S., 2012, "Zeolite Rho: A Highly Selective Adsorbent for Co2/Ch4 Separation Induced by a Structural Phase Modification," Chemical Communications, 48(2), pp. 215-217.

[3] Süer, M. G., Baç, N., and Yilmaz, L., 1994, "Gas Permeation Characteristics of Polymer-Zeolite Mixed Matrix Membranes," Journal of Membrane Science, 91(1–2), pp. 77-86.

[4] Zimmerman, C. M., Singh, A., and Koros, W. J., 1997, "Tailoring Mixed Matrix Composite Membranes for Gas Separations," Journal of Membrane Science, 137(1–2), pp. 145-154.

[5] Ismail, A. F., and David, L. I. B., 2001, "A Review on the Latest Development of Carbon Membranes for Gas Separation," Journal of Membrane Science, 193(1), pp. 1-18.

[6] Bara, J. E., Hatakeyama, E. S., Gin, D. L., and Noble, R. D., 2008, "Improving Co2 Permeability in Polymerized Room-Temperature Ionic Liquid Gas Separation Membranes through the Formation of a Solid Composite with a Room-Temperature Ionic Liquid," Polymers for Advanced Technologies, 19(10), pp. 1415-1420.

[7] Marzouk, S. a. M., Al-Marzouqi, M. H., El-Naas, M. H., Abdullatif, N., and Ismail, Z. M., 2010, "Removal of Carbon Dioxide from Pressurized CO_2–CH_4 Gas Mixture Using Hollow Fiber Membrane Contactors," Journal of Membrane Science, 351(1–2), pp. 21-27.

[8] Francisco, G. J., Chakma, A., and Feng, X., 2010, "Separation of Carbon Dioxide from Nitrogen Using Diethanolamine-Impregnated Poly(Vinyl Alcohol) Membranes," Separation and Purification Technology, 71(2), pp. 205-213.

[9] Iarikov, D. D., Hacarlioglu, P., and Oyama, S. T., 2011, "Supported Room Temperature Ionic Liquid Membranes for Co2/Ch4 Separation," Chemical Engineering Journal, 166(1), pp. 401-406.

[10] Pathare, R., and Agrawal, R., 2010, "Design of Membrane Cascades for Gas Separation," Journal of Membrane Science, 364(1–2), pp. 263-277.

[11] Karode, S. K., and Kumar, A., 2001, "Flow Visualization through Spacer Filled Channels by Computational Fluid Dynamics I.: Pressure Drop and Shear Rate Calculations for Flat Sheet Geometry," Journal of Membrane Science, 193(1), pp. 69-84.

[12] Wiley, D. E., and Fletcher, D. F., 2003, "Techniques for Computational Fluid Dynamics Modelling of Flow in Membrane Channels," Journal of Membrane Science, 211(1), pp. 127-137.

[13] Villaluenga, J. P. G., and Cohen, Y., 2005, "Numerical Model of Non-Isothermal Pervaporation in a Rectangular Channel," Journal of Membrane Science, 260(1–2), pp. 119-130.

[14] Ma, S., and Song, L., 2006, "Numerical Study on Permeate Flux Enhancement by Spacers in a Crossflow Reverse Osmosis Channel," Journal of Membrane Science, 284(1–2), pp. 102-109.

[15] Fimbres-Weihs, G. A., Wiley, D. E., and Fletcher, D. F., 2006, "Unsteady Flows with Mass Transfer in Narrow Zigzag Spacer-Filled Channels: A Numerical Study," Industrial & Engineering Chemistry Research, 45(19), pp. 6594-6603.

[16] Subramani, A., Kim, S., and Hoek, E. M. V., 2006, "Pressure, Flow, and Concentration Profiles in Open and Spacer-Filled Membrane Channels," Journal of Membrane Science, 277(1–2), pp. 7-17.

[17] Fimbres-Weihs, G. A., and Wiley, D. E., 2007, "Numerical Study of Mass Transfer in Three-Dimensional Spacer-Filled Narrow Channels with Steady Flow," Journal of Membrane Science, 306(1–2), pp. 228-243.

[18] Lyster, E., and Cohen, Y., 2007, "Numerical Study of Concentration Polarization in a Rectangular Reverse Osmosis Membrane Channel: Permeate Flux Variation and Hydrodynamic End Effects," Journal of Membrane Science, 303(1–2), pp. 140-153.

[19] Fimbres-Weihs, G. A., and Wiley, D. E., 2008, "Numerical Study of Two-Dimensional Multi-Layer Spacer Designs for Minimum Drag and Maximum Mass Transfer," Journal of Membrane Science, 325(2), pp. 809-822.

[20] Pal, S., Bharihoke, R., Chakraborty, S., Ghatak, S. K., De, S., and Dasgupta, S., 2008, "An Experimental and Theoretical Analysis of Turbulence Promoter Assisted Ultrafiltration of Synthetic Fruit Juice," Separation and Purification Technology, 62(3), pp. 659-667.

[21] Shakaib, M., Hasani, S. M. F., and Mahmood, M., 2009, "Cfd Modeling for Flow and Mass Transfer in Spacer-Obstructed Membrane Feed Channels," Journal of Membrane Science, 326(2), pp. 270-284.

[22] Marcos, B., Moresoli, C., Skorepova, J., and Vaughan, B., 2009, "CFD Modeling of a Transient Hollow Fiber Ultrafiltration System for Protein Concentration," Journal of Membrane Science, 337(1–2), pp. 136-144.

[23] Fletcher, D. F., and Wiley, D. E., 2004, "A Computational Fluids Dynamics Study of Buoyancy Effects in Reverse Osmosis," Journal of Membrane Science, 245(1–2), pp. 175-181.

[24] Alkhamis, N., Anqi, A., Oztekin, D.E., Alsaiari, A. and Oztekin, A. “Gas Separation using a Membrane” *Proceeding of ASME-IMECE2013-San Diego* (2013)